Eur. Phys. J. B **29**, 419–424 (2002)
DOI: 10.1140/epjb/e2002-00324-5

THE EUROPEAN PHYSICAL JOURNAL B

Magnetization and resistivity steps in the phase separated $Pr_{0.5}Ca_{0.5}Mn_{1-x}Ni_xO_3$ manganites

S. Hébert[1], A. Maignan[1,a], V. Hardy[1], C. Martin[1], M. Hervieu[1], B. Raveau[1], R. Mahendiran[2], and P. Schiffer[2]

[1] Laboratoire CRISMAT, ISMRA, 6 Boulevard du Maréchal Juin 14050 Caen Cedex, France
[2] Department of Physics and Materials Research Institute, 104 Davey Laboratory, Pennsylvania State University, University Park, PA-16802, USA

Received 5 April 2002 / Received in final form 8 July 2002

Abstract. The low temperature magnetic and transport properties of the $Pr_{0.5}Ca_{0.5}Mn_{1-x}Ni_xO_3$ manganites ($0 \leq x \leq 0.1$) have been investigated. The presence of Ni hinders the charge and orbital ordering observed in $Pr_{0.5}Ca_{0.5}MnO_3$ and favors the creation of ferromagnetic regions, leading to phase separation. The ferromagnetic fractions induced by the Ni substitution have been estimated from magnetization measurements, they are large and reach 40% for 4% of Ni. Steps are observed in the $M(H)$ and $\rho(H)$ curves of all the samples at $T < 5$ K. They are similar to the steps observed in $Pr_{0.5}Ca_{0.5}Mn_{1-x}M_xO_3$, where M is a non magnetic cation (Mg^{2+}, Ga^{3+},...), and for which the ferromagnetic fractions are very small (less than 2%), however, their appearance is restricted to lower temperatures ($T < 5$ K) with Ni dopant than with non magnetic cations. This study shows that steps can be observed in a wide range of phase-separated systems, even when the ferromagnetic fraction is very large.

PACS. 71.30.+h Metal-insulator transitions and other electronic transitions – 75.25.+z Spin arrangements in magnetically ordered materials (including neutron and spin-polarized electron studies, synchrotron-source X-ray scattering, etc.) – 61.14.-x Electron diffraction and scattering

Manganites $Ln_{1-x}Ae_xMnO_3$ have been the subject of intense studies in recent years after the discovery of colossal magnetoresistance (CMR) property ([1] and Refs. therein). In these compounds, the Mn^{3+}/Mn^{4+} ions are linked through double-exchange interactions which favour the hopping of the e_g electrons when the Mn core spins are aligned. The application of a magnetic field leads, therefore, to a drastic reduction of resistivity. For $Pr_{0.5}Ca_{0.5}MnO_3$, the double-exchange is hindered by the establishment of long range charge-ordering and orbital-ordering (CO/OO) [2] at $T_{CO} \sim 250$ K for the Mn^{3+}/Mn^{4+} ratio equal to 1. This antiferromagnetic CO/OO phase is very stable and a magnetic field of 27 T is required at 4.2 K to melt it into a ferromagnetic metallic (FMM) state [3].

One way to destabilize CO/OO is to partially substitute Mn by a foreign cation [4]. Two different behaviours can be found depending on the cation, as summarized in reference [5]. Di-, tri-, tetra- or pentavalent non magnetic cations, *i.e.* with d^0 or d^{10} electronic configurations, can destabilize CO/OO and favor insulator to metallic (I/M) transition in the presence of magnetic field, while magnetic cations (except Fe^{3+}) such as Cr^{3+}, Co^{2+} induce the formation of large ferromagnetic fractions with I/M transitions even without magnetic field. Ni^{2+} is one of those cations [6], yielding a maximum magnetic moment of 2.6 μ_B in 1.45 T and a maximal T_C close to 75 K for 4% of Ni. In these substituted compounds, phase separation is induced and CO/OO short range AFM regions are found to coexist with charge disordered FMM zones as evidenced by Electron Microscopy and Neutron Powder Diffraction (NPD) studies [7]. The size of the CO/OO areas determined by electron microscopy at 92 K is close to 10–100 nm as observed in $Pr_{0.5}Ca_{0.5}Mn_{0.95}Al_{0.05}O_3$ [7] and $Pr_{0.5}Ca_{0.5}Mn_{0.95}Ga_{0.05}O_3$ [8].

The existence of phase separation can induce very peculiar behaviours for a narrow range of doping. The influence of thermal cycling has been investigated by Mahendiran *et al.* in these compounds, doped with a maximum of 3% of Cr, Ni or Al [9]: this thermal treatment induces a spectacular increase of resistivity and a decrease of magnetization associated with the stabilization of CO/OO phase by thermal cycling at the expense of the FM one. One new puzzling phenomenon has been recently observed: it has been found that at low temperatures ($T < 10$ K), the magnetic field driven magnetization curves exhibit steep jumps on the increasing branch, which are also observed in resistivity and specific heat

---

[a] e-mail: `antoine.maignan@ismra.fr`

measurements [8]. The magnetization increases by several steps, in some cases up to the expected saturation value (for example in $Pr_{0.5}Ca_{0.5}Mn_{0.95}Ga_{0.05}O_3$ [10,11]), and the transition is irreversible. As specific heat measurements also exhibit these steep jumps, it was argued that they could not simply be related to a reorientation of magnetic domains but rather to a magnetic phase transition from AFM to FM [8]. These jumps have been observed in a large number of Mn site substituted $Pr_{0.5}Ca_{0.5}Mn_{1-x}M_xO_3$, where M is a non magnetic cation (Mg^{2+}, Ga^{3+}, Ti^{4+}, Sn^{4+} etc). The substitution destabilizes the CO/OO phases, induces phase separation, and jumps in the $M(H)$ curves are observed [10]. For these non magnetic dopants, the ferromagnetic fraction was estimated to be rather small (maximum 2%). We report here results obtained for the $Pr_{0.5}Ca_{0.5}Mn_{1-x}Ni_xO_3$ series with $0 \leq x \leq 0.1$, a family in which large ferromagnetic fractions are evidenced and for which metal to insulator transitions are observed even without applied field.

The $Pr_{0.5}Ca_{0.5}Mn_{1-x}Ni_xO_3$ manganites were prepared in the form of polycrystalline samples by mixing the oxides Pr_6O_{11}, CaO, MnO_2 and NiO in stoichiometric proportions. The powders, first heated at 1000 °C, were pressed in the form of bars of typical dimensions $2 \times 2 \times 10$ mm. The sintering was made at 1200 °C and at 1500 °C for 12 h, then the samples were slowly cooled down to 800 °C and quenched to room temperature. To ensure that the final quench has no impact on the step features under study, two compositions, $x = 0.04$ and $x = 0.08$, were also slowly cooled down (10 °C/h from 800 °C). Their magnetization steps are found to exhibit similar features to that of quenched ceramics. Another evidence against a determinant role of the quench is that magnetization steps are also observed in crystals grown by the floating zone method, *i.e.* a completely different technique.

The purity of the samples was checked by X-ray powder diffraction and by electron microscopy (electron diffraction (ED)) and their compositional homogeneity was examined by Energy Dispersive Spectroscopy (EDS) coupled to ED. For all studied x values, a clear correspondence between the nominal and actual Ni contents is observed in the accuracy limit of the technique (±0.01). This result rules out any 'chemical' phase separation which could be responsible for the step feature at 2.5 K described hereafter. Since the CO/OO observations by electron microscopy (ED) cannot be performed below 92 K with our set-up, any comparisons with magnetic properties (2.5 K) is delicate. Only the $x = 0.10$ composition, corresponding to the largest Ni content of the series has been studied at 92 K by ED. A more complete structural study for other x is now under progress and will be reported separately.

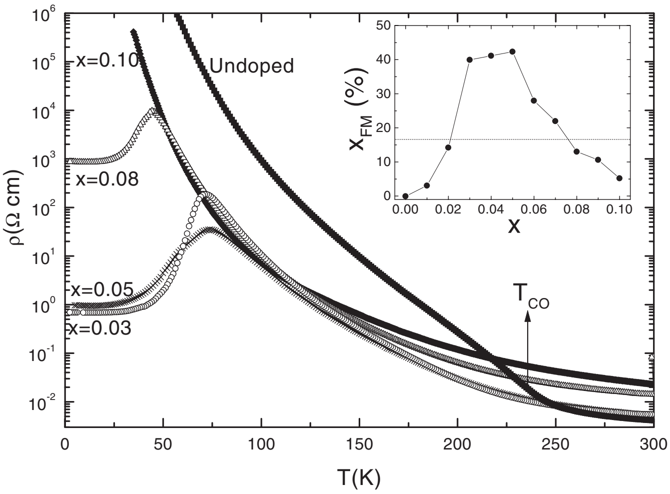

Fig. 1. $\rho(T)$ of $Pr_{0.5}Ca_{0.5}Mn_{1-x}Ni_xO_3$ measured in 0 T. Inset: Ferromagnetic fraction x_{FM} as a function of x, estimated from the magnetization measured at 5 K and 0.2 T: $x_{FM} = (M - M_{undoped})/M_{Ru0.05}$.

The physical properties have been measured using a SQUID magnetometer for magnetization studies and a Physical Properties Measurements System for transport measurements (four probe resistivity), both from Quantum Design. Previous measurements have shown that the measurements are highly sensitive to the thermal and magnetic field history of the sample. Therefore a 'virgin' piece of ceramic was selected for each $M(H)$ or $\rho(H)$ measurement.

Figure 1 presents the resistivity ρ measured under 0 T as a function of temperature for the $Pr_{0.5}Ca_{0.5}Mn_{1-x}Ni_xO_3$ series with $0 \leq x \leq 0.1$. ρ is strongly decreased below T_{CO} by the introduction of Ni on the Mn site and the change of slope at $T_{CO} \sim 250$ K, characteristic of CO/OO observed for the undoped compound, has been suppressed. At room temperature, ρ increases as the Ni content increases, as expected from the increase of disorder in the Mn network. As T decreases, an insulator-to-metal transition (I/M) occurs for Ni content as small as $x \sim 0.03$. The resistivity at 5 K, $\rho_{5\,K}$, is minimal for $x \sim 0.03$ and then increases as x increases. For $x > 0.08$, the I/M transition disappears, the sample is insulating in the whole temperature range with a resistivity at low T still much smaller than the one of the undoped compound (for example, at 50 K, $\rho = 10^4\ \Omega\,$cm for $x = 0.1$ while $\rho > 10^6\ \Omega\,$cm for $x = 0$).

The inset of Figure 1 presents the ferromagnetic fraction x_{FM} estimated from the $M(H)$ loops measured at 2.5 K. Following previous studies [12], x_{FM} has been estimated at 2.5 K in a field of 0.2 T assuming that this small field will favor FM alignment of domains without influencing the CO/OO to FM transition. x_{FM} is equal to the ratio of the magnetic moment measured at 2.5 K and 0.2 T (corrected from the value of magnetization in the undoped compound) divided by the moment of $Pr_{0.5}Ca_{0.5}Mn_{0.95}Ru_{0.05}O_3$, for which a fraction of ferromagnetic regions of 100% is assumed [5]. In the inset of Figure 1, the theoretical 3D percolation threshold, 17%, is represented by the dotted line, and consistently with the $\rho(T)$ measurements, the inset shows that an I/M transition should exist for x ranging from $x \sim 0.02$ to $x \sim 0.08$. Taking the uncertainty on the determination of x_{FM} into account, the good agreement between the estimated x_{FM} and the $\rho(T)$ curves is highly satisfactory in the framework

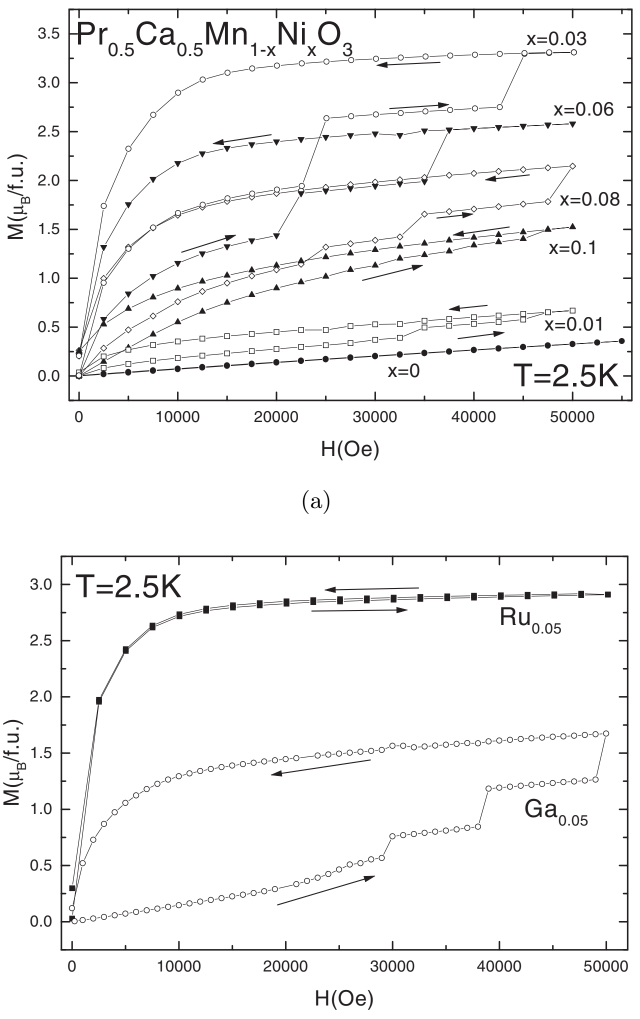

(a)

(b)

Fig. 2. a) $M(H)$ loops at $T = 2.5$ K of $Pr_{0.5}Ca_{0.5}Mn_{1-x}Ni_xO_3$. b) $M(H)$ loops at $T = 2.5$ K of $Pr_{0.5}Ca_{0.5}Mn_{0.95}Ga_{0.05}O_3$ and $Pr_{0.5}Ca_{0.5}Mn_{0.95}Ru_{0.05}O_3$.

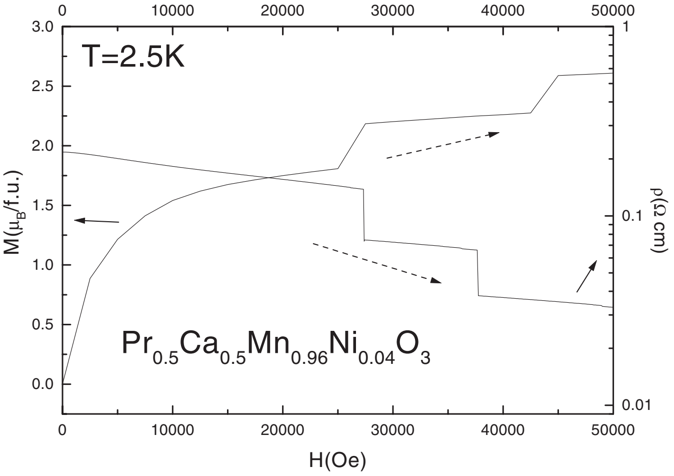

Fig. 3. $M(H)$ (left-scale) and $\rho(H)$ (right-scale) at 2.5 K of $Pr_{0.5}Ca_{0.5}Mn_{0.96}Ni_{0.04}O_3$.

of the percolation scenario. Since the Ni^{2+} substitution for manganese generates Mn^{3+}/Mn^{4+} ferromagnetic metallic regions in the CO/OO matrix, an I/M transition is expected as soon as x_{FM} becomes larger than the percolation threshold. Nonetheless, large concentrations of Ni^{2+} (like 10%) shifts significantly the Mn valency towards 4+ which tends to reinforce the Mn^{3+}/Mn^{4+} CO/OO phenomena at the expense of the FM state. Moreover, Ni^{2+} (or Co^{2+}) exhibit different electronic configurations than those of Mn^{3+}/Mn^{4+}. This is not the case of chromium, Mn^{4+} and Cr^{3+} being isoelectronic. Consequently, the Ni^{2+} participation to the Mn^{3+}/Mn^{4+} double-exchange process is not as good as that of Cr^{3+}. By increasing too much the Ni concentration, the FM state becomes diluted and consequently this will also favor a decrease of the FM fraction. This gives a rough explanation for the existence of an optimum in the FM fraction as a function of Ni concentration.

Figure 2 presents the $M(H)$ loops measured at 2.5 K for different Ni concentrations. As x increases, the magnetization increases and reaches a maximum for $x = 0.03$, with M reaching the maximal value $M = 3.3\mu_B$ at 5 T. The magnetization curve is not continuous as H increases, but presents steps, similar to the ones encountered in $Pr_{0.5}Ca_{0.5}Mn_{1-x}M_xO_3$, where x is a non magnetic cation. An example of the $M(H)$ loops obtained in $Pr_{0.5}Ca_{0.5}Mn_{0.95}Ga_{0.05}O_3$ is shown in Figure 2b. For comparison, the $M(H)$ loop obtained in the 100% ferromagnetic Ru doped sample is also shown: no steps are observed in the whole field range.

Steps appear for Ni concentration as small as $x = 0.01$. For $x = 0.03$, two steps are necessary to reach saturation, at 2.25 T and 4.25 T. As the Ni concentration increases beyond 0.03, magnetization decreases again, but steps are still observed up to $x = 0.1$. The magnetic fields H_s where steps are observed depend on x: for $x \leq 0.06$, H_s decreases as x increases (2 T and 3.5 T for $x = 0.06$ compared to 2.5 T and 4 T for $x = 0.01$) whereas for $x > 0.06$, H_s increases with x (2.25 T, 3.25 T and 4.75 T for $x = 0.08$). The size of the jumps is close to 0.1–0.2μ_B for $x < 0.03$, increases to 0.3–0.5μ_B for $x \leq 0.07$, with a maximum of 0.7μ_B for $x = 0.03$, and starts to decrease for $x > 0.07$. From all the investigated curves, it seems that the appearance of jumps does not correspond to a critical value of magnetization and/or field, as previously reported also for the non-magnetic cations case [8,10]. Moreover, in the case of non-magnetic cations, the x_{FM} values estimated from the M-H loops were always very small (<2%), whereas, in the case of Ni, it evolves from 3% to 40% and steps are also observed in the whole investigated range.

Steps are also observed on the field dependent resistivity curves. Figure 3 shows the comparison between the $M(H)$ and $\rho(H)$ curves for $x = 0.04$ for the increasing field branch. Two jumps are observed on the $M(H)$ curve, corresponding to two jumps on the $\rho(H)$ curve. The positions of the first jump are in good coincidence but the second step is located at a lower field on the $\rho(H)$ than on the $M(H)$ curve. Even if there exists some agreement between the two curves, a perfect correspondence in the position of steps is not expected as the two techniques probe

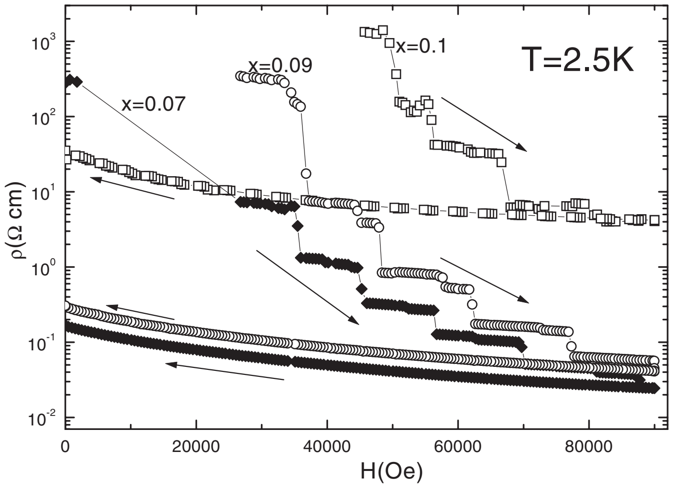

Fig. 4. $\rho(H)$ at $T = 2.5$ K of $Pr_{0.5}Ca_{0.5}Mn_{1-x}Ni_xO_3$, with $x = 0.07$; 0.09 and 0.1.

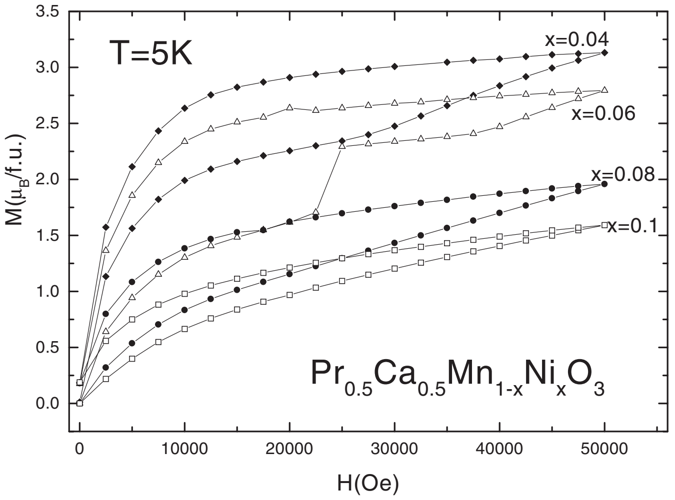

Fig. 5. $M(H)$ loops at $T = 5$ K of $Pr_{0.5}Ca_{0.5}Mn_{1-x}Ni_xO_3$.

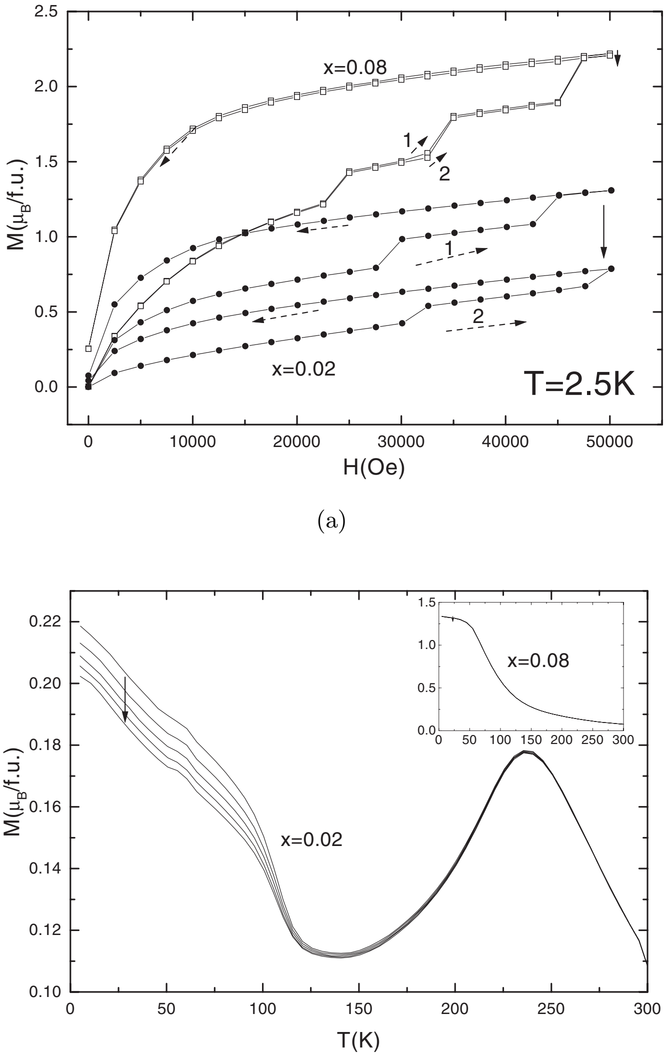

(a)

(b)

Fig. 6. a) Two successive $M(H)$ loops recorded at 2.5 K for $x = 0.02$ and $x = 0.08$. The samples have been warmed at 300 K between the two loops. b) Five (three) successive $M(T)$ recorded under 1.45 T for $x = 0.02$ (for $x = 0.08$). The samples have first been field cooled down to 5 K.

different time scales and correspond to different sweep rates for the application of magnetic field [8,10]. Figure 4 presents the $\rho(H)$ curves for $x = 0.07$, 0.09 and 0.1 at $T = 2.5$ K. Steps are observed for the three samples, and the characteristic fields of steps increase as the Ni content increases, as previously inferred from the $M(H)$ curves.

Figure 5 presents the $M(H)$ loops measured at 5 K. One step is observed in the $x = 0.06$ case at 2.25 T, a field larger than the position of the first step at 2.5 K. For $x \leq 0.05$, there is only a change of slope in the $M(H)$ curve instead of steps at ~2.5 T. The results presented in Figure 5 are thus different from the case of non magnetic cations: for the former, jumps were observed for $T \leq 10$ K [8,10] while in the case of Ni doping, the temperature range where these jumps are observed is more limited, as they have disappeared at 5 K.

The $M(H)$ curves, especially the position and size of steps, can be very sensitive to the thermal history of the samples [8,10,11]. Two successive $M(H)$ loops recorded at 2.5 K for $x = 0.02$ and $x = 0.08$ are presented in Figure 6a. For both compositions, the ferromagnetic fraction x_{FM} estimated after the first zero field cooling is close to 15%, as shown in Figure 1. After the first loop, the samples have been warmed up to 300 K and cooled down again to 2.5 K. For $x = 0.02$, the position of the steps is shifted to higher fields after thermal cycling. This effect was also observed in the case of $Pr_{0.5}Ca_{0.5}Mn_{1-x}M_xO_3$ when M is a non magnetic cation [8,10]. Furthermore, for magnetic field values below the first step, the magnetization decreases after thermal cycling, which corresponds to a decrease of x_{FM}. Similar results are obtained for all the compounds with $x < 0.06$: the thermal cycling seems to prevent the establishment of ferromagnetism in these compounds, and stabilize the CO/OO phase, thus delaying the appearance of steps to higher magnetic fields. On the other hand, for $x = 0.08$, the two increasing magnetization curves are superimposed up to the field where jumps are observed, *i.e.* x_{FM} determined at 0.2 T is not affected by the cycling. Also the position and size of jumps is almost unaffected by the thermal cycling. Thermal cycling effect can also be evidenced on the $M(T)$ curves. Figure 6b presents the $M(T)$ curves measured after cooling in a field of 1.45 T and warming the samples to 300 K between each $M(T)$. Cycling the sample up to 300 K results in a spectacular decrease of M in the following measurements in the case $x = 0.02$ as previously reported in Cr or Al doped samples [9], but on the other hand, the successive $M(T)$ curves registered for $x = 0.08$ are superimposed, the thermal cycling effect has completely disappeared. However, this difference of behaviour with respect to thermal cycling does not affect the existence of jumps: they are observed in the two sets of samples, for all the x investigated.

The comparison of the results obtained on Ni doped samples with those previously reported on $\mathrm{Pr_{0.5}Ca_{0.5}Mn_{1-x}M_xO_3}$ (M=Mg, Ga, Sn, Sc....[8,10,11]) leads to the following remarks:
(i) The temperature range where jumps are observed (for $H < 50\,000$ Oe) with Ni is restricted to lower temperatures compared to the case of non magnetic dopants.
(ii) The ferromagnetic fraction x_{FM} in the Ni doped samples exhibiting jumps can be much larger than for non magnetic dopants, reaching 40%.
iii) The size and the position in fields of the jumps are rather similar for Ni and non-magnetic cations, close to 0.3–0.5μ_B but larger steps magnitude of 1.7–1.8μ_B have been observed only in the case of non-magnetic cations [10], for which x_{FM} before the jump is much smaller than in the case of Ni doping.
(iv) The doping content for which jumps are observed can be as large as 10% of Ni while, for non magnetic dopant, they mostly appear for 3–5% and then they disappear beyond these values.
(v) The low field behaviour of $\mathrm{Pr_{0.5}Ca_{0.5}Mn_{1-x}Ni_xO_3}$ depends on whether $x < 0.06$ or $x > 0.06$ but this difference does not affect the steps.

A key parameter for the observation of these jumps is the phase separation. In the case of the purely AFM or FM compounds, no steps are observed. For the undoped AFM $\mathrm{Pr_{0.5}\ Ca_{0.5}MnO_3}$, only a metamagnetic transition is observed at low temperature for a field close to 27 T [3]. For the ferromagnetic Ru doped sample $\mathrm{Pr_{0.5}Ca_{0.5}Mn_{0.95}Ru_{0.05}O_3}$ [5], the $M(H)$ loops show no jump down to 2.5 K and the first magnetization curve is very steep, with M reaching $2\mu_B$ for a field as small as 2500 Oe even at $T = 2.5$ K (Fig. 2b).

The formation of these jumps in the $\mathrm{Pr_{0.5}Ca_{0.5}Mn_{1-x}M_xO_3}$ system (with M=Ga, Mg....[8, 10,11]) has been interpreted in the framework of the martensitic transformation [11]. In the martensitic systems, the high temperature austenite phase transforms into the martensite phase as T decreases. Although the transition is of first order, multi-step transformations can be obtained because of a too large elastic energy term created by the strain between the two phases [13]. For the $\mathrm{Pr_{0.5}Ca_{0.5}Mn_{1-x}M_xO_3}$ system, the phase transformation is induced by the magnetic field and the ferromagnetic phase corresponds to the low T martensite phase, while the low field CO/OO AFM phase (with a strong structural distorsion) corresponds to the high T austenite.

In the case of Ni doping, a similar explanation for the appearance of jumps can be proposed but the nature of the low field phase has to be clarified. The main difference compared to the previous studies is that the ferromagnetic fraction x_{FM} in this low field region is already much larger than what was obtained with Ga, Mg etc. The value of x_{FM} increases indeed very rapidly with the Ni content, reaching a maximum of 40% for $x = 0.04$, compared to a maximum of 2.3% obtained with 5% of Ga [10]. The role of Ni is first to destabilize CO/OO as such a divalent foreign cation destroys the ordering of $\mathrm{Mn^{3+}/Mn^{4+}}$. Moreover, contrary to the case of non magnetic cations, the e_g levels of $\mathrm{Ni^{2+}}$ with electronic configuration $3d^8$ can participate to the band formation and favor metallicity, so that 3% of Ni only is sufficient to induce an I/M transition. Larger contents of Ni result in a decrease of x_{FM} possibly due to the progressive dilution of the magnetic interactions between $\mathrm{Mn^{3+}}$ and $\mathrm{Mn^{4+}}$. Also for $x > 0.06$, the thermal cycling effect disappears, reflecting the fact that the nature of the low field phase is most probably different for $x < 0.06$ and $x > 0.06$.

The structure of $\mathrm{Pr_{0.5}Ca_{0.5}Mn_{1-x}M_xO_3}$ has been investigated by Electron Microscopy and Neutron Powder Diffraction for M=Cr and Al [7] and $x = 0.05$. In the 5% Cr doped samples (with x_{FM} close to 100% [5]), NPD investigation reveals the presence of a unique long range ferromagnetic phase at low temperature (5 K) even if electron microscopy investigation at 92 K shows that small short-range CO/OO regions still exist. For the 5% Al doped samples, the situation is more complex: the AFM state is badly established and the NPD patterns are refined with two crystalline and two magnetic phases but no long range FM is evidenced. The electron microscopy confirms the presence of short-range CO/OO regions at 92 K. The 5% Co doped samples have also been investigated by NPD [14]: a ferromagnetic phase is evidenced at low T, with a smaller moment than in the case of Cr ($\approx 1.5\mu_B$). Susceptibility and thermopower measurements have shown that CO/OO is weakened but still present for 5% of Co [5]. Doping with Ni induces the same behaviour as with Co doping as shown by magnetic and transport measurements [5]: the low field phase for $x < 0.06$ would thus consist of long-range ordered ferromagnetic regions mixed with short-range AFM distorted CO/OO regions. On the other hand, electron microscopy shows at 92 K that CO/OO has been suppressed with 10% of Ni. However, this does not rule out the possibility that phase separation persists and that two magnetic phases with different cell parameters still coexist at very low temperatures for $x > 0.06$ and favor the occurrence of jumps.

In conclusion, the present study demonstrates the existence of an optimum in the ferromagnetic metallic fraction induced by Ni for Mn substitution in

$Pr_{0.5}Ca_{0.5}Mn_{1-x}Ni_xO_3$. This fraction reaches a maximum of about 40% for x values around 0.04. For $0.03 \leq x \leq 0.07$, *i.e.* all the compositions beyond the 3D percolation threshold, 17%, an insulator to metal transition is observed as T decreases from RT. The observation of steps on the magnetization and resistivity curves *versus* magnetic field, at 2.5 K, for all the compositions ($0.01 \leq x \leq 0.10$) shows for the first time that a large ferromagnetic fraction is also compatible with this feature. It is also found that the thermal cycling effect induces or not modifications in the steps, depending on the Ni concentration with respect to the optimum ones. To understand the exact role of the phase separation upon the steps generation, a structural study at 4.2 K for different concentrations of impurity is now under progress.

The work of Penn State authors are supported NSF grant DMR -0101318. R. Mahendiran also acknowledges MNERT (France) for financial assistance.

References

1. *Colossal Magnetoresistance, Charge Ordering and Related Properties of Manganses Oxides*, edited by C.N.R. Rao, B. Raveau (World Scientific, Singapore, 1998); *Colossal Magnetoresistance Oxides*, edited by Y. Tokura (Gordon and Breach, London 1999)
2. E.O. Wollan, W.C. Koehler, Phys. Rev. **100**, 545 (1955); J.B. Goodenough, Phys. Rev. **100**, 564 (1955); Z. Jirak, S. Krupicka, Z. Simsa, M. Dlouha, S. Vratislav, J. Magn. Magn. Mater. **53**, 153 (1985)
3. M. Tokunaga, N. Miura, Y. Tomioka, Y. Tokura, Phys. Rev. B **57**, 5259 (1998)
4. B. Raveau, A. Maignan, C. Martin, M. Hervieu, J. Solid State Chem. **130**, 162 (1997); A. Maignan, F. Damay, A. Barnabé, C. Martin, M. Hervieu, B. Raveau, Philos. Trans. R. Soc. Lond., Ser. A **356**, 1635 (1998); P.V. Vanitha, A. Arulraj, A.R. Raju, C.N.R. Rao, C.R. Acad. Sci. **2** (serie IIc), 595 (1999); T. Kimura, Y. Tomioka, Y. Tokura, Phys. Rev. Lett. **83**, 3940 (1999)
5. S. Hébert, A. Maignan, C. Martin, B. Raveau, Solid State Comm. **121**, 229 (2002), and references therein
6. A. Maignan, F. Damay, C. Martin, B. Raveau, Mat. Res. Bull. **32**, 965 (1997)
7. C. Martin, A. Maignan, F. Damay, M. Hervieu, B. Raveau, Z. Jirak, G. André, F. Bourée, J. Magn. Magn. Mater. **202**, 11 (1999)
8. S. Hébert, V. Hardy, A. Maignan, R. Mahendiran, M. Hervieu, C. Martin, B. Raveau, J. Solid State Chem. **165**, 6 (2002)
9. R. Mahendiran, A. Maignan, M. Hervieu, C. Martin, B. Raveau, J. Appl. Phys. **90**, 2422 (2001)
10. S. Hébert, A. Maignan, V. Hardy, C. Martin, M. Hervieu, B. Raveau, Solid Stat. Comm. **122**, 335 (2002)
11. V. Hardy, S. Hébert, A. Maignan, C. Martin, M. Hervieu, B. Raveau, submitted to Phys. Rev. B.
12. K.H. Kim, M. Uehara, C. Hess, P.A. Sarma, S.W. Cheong, Phys. Rev. Lett. **84**, 2961 (2000)
13. E. Vives, J. Ortin, L. Manosa, I. Rafols, R. Pérez-Magrané, A. Planes, Phys. Rev. Lett. **72**, 1694 (1994)
14. R. Mahendiran *et al.*, unpublished